

# The PriA Replication Restart Protein Blocks Replicase Access Prior to Helicase Assembly and Directs Template Specificity through Its ATPase Activity<sup>\*[5]</sup>

Received for publication, November 12, 2012, and in revised form, December 19, 2012. Published, JBC Papers in Press, December 21, 2012, DOI 10.1074/jbc.M112.435966

Carol M. Manhart and Charles S. McHenry<sup>1</sup>

From the Department of Chemistry and Biochemistry, University of Colorado, Boulder, Colorado 80303

**Background:** PriA initiates restart at stalled replication forks.

**Results:** A FRET assay detects *E. coli* and *B. subtilis* PriA-mediated helicase loading.

**Conclusion:** PriA ATPase activity directs specificity toward larger gaps on leading strands. PriA blocks replicase binding.

**Significance:** This work reveals a novel role of an ATPase in regulating DNA structural specificity and establishes the mechanism of PriA as a checkpoint protein.

The PriA protein serves as an initiator for the restart of DNA replication on stalled replication forks and as a checkpoint protein that prevents the replicase from advancing in a strand displacement reaction on forks that do not contain a functional replicative helicase. We have developed a primosomal protein-dependent fluorescence resonance energy transfer (FRET) assay using a minimal fork substrate composed of synthetic oligonucleotides. We demonstrate that a self-loading reaction, which proceeds at high helicase concentrations, occurs by threading of a preassembled helicase over free 5'-ends, an event that can be blocked by attaching a steric block to the 5'-end or coating DNA with single-stranded DNA binding protein. The specificity of PriA for replication forks is regulated by its intrinsic ATPase. ATPase-defective PriA K230R shows a strong preference for substrates that contain no gap between the leading strand and the duplex portion of the fork, as demonstrated previously. Wild-type PriA prefers substrates with larger gaps, showing maximal activity on substrates on which PriA K230R is inactive. We demonstrate that PriA blocks replicase function on forks by blocking its binding.

In bacteria, DNA replication initiates at a unique chromosomal origin directed by sequence-specific binding of multiple copies of DnaA with ensuing loading of the replicative helicase by a helicase loader (1, 2). Once replication forks are established, they often encounter a block before they reach DNA replication termination points, roughly 2 mega base pairs away on the *Escherichia coli* chromosome (3). Once the replisome dissociates, DnaA no longer functions to re-establish the replication fork. This reaction is driven by the PriA protein in both Gram-negative and Gram-positive model organisms, *E. coli* and *Bacillus subtilis* (4, 5).

In *E. coli*, several proteins are thought to act sequentially in building up the apparatus that can attract the helicase loader

and assemble an active replication fork. Gel shift assays indicate that PriA binds initially, followed by PriB and then DnaT (6). The resulting complex recruits the *E. coli* helicase loader/helicase (DnaC/DnaB), leading to helicase assembly in the presence of ATP (6).

Thus, PriA appears to be the lead protein that directs assembly of the restart primosome. This is consistent with its substrate specificity in binding to D loops, but not bubbles, and three-stranded structures that provide models for replication forks (7, 8). PriA contains an intrinsic 3'-5' helicase that has been suggested to function to clear an annealed lagging strand product from the replication fork, creating a site for primosome assembly and helicase loading (9, 10). However, PriA mutants that are defective in helicase activity remain active and are even more effective than their wild-type counterparts on substrates containing single-stranded lagging strands (11). This has been proposed to be due to the mutant form remaining resident at the fork and not migrating away. PriA has also been shown to be a checkpoint protein that blocks the intrinsic strand displacement activity of DNA polymerase III holoenzyme (Pol III HE)<sup>2</sup> on forks before an active replicative helicase has been assembled (12, 13).

Early in the primosome assembly reaction, a handoff mechanism has been proposed, sequentially, between PriA, PriB and DnaT. Weak PriA-PriB and PriB-DnaT interactions are strengthened in the presence of single-stranded DNA. The binding sites on single-stranded DNA are partially shared by PriA, PriB, and DnaT. It has been suggested that the primosome assembly process is a dynamic one in which these proteins hand off the fork substrate to one another, culminating with DnaT binding to PriB and displacing it from DNA to provide a landing site for the helicase loader and helicase (14).

A replication restart protein-initiated rolling circle replication system has been established for *E. coli* that recapitulates the rate observed for replication forks *in vivo* (15, 16). Using this system, many of the basic principles of fork dynamics have been

\* This work was supported by Grant MCB-0919961 from the National Science Foundation.

[5] This article contains supplemental Table S1 and Figs. S1–S5.

<sup>1</sup> To whom correspondence should be addressed: Dept. of Chemistry and Biochemistry, University of Colorado, 3415 Colorado Ave., UCBS96, Boulder, CO 80303. E-mail: charles.mchenry@colorado.edu.

<sup>2</sup> The abbreviations used are: Pol III HE, DNA polymerase III holoenzyme; PolC HE, PolC holoenzyme (a combination of *B. subtilis* PolC,  $\beta$ , and  $\tau$ -complex); nt, nucleotide; DnaE HE (a combination of *B. subtilis* DnaE,  $\beta_2$ , and  $\tau$ -complex); SSB, single-stranded DNA binding protein.

## PriA Specificity and Function

established, including the reversible association of primase with the replicative helicase, regulating Okazaki fragment length (16, 17) and the association of the  $\tau$ -subunit of the Pol III holoenzyme with the replicative helicase. The latter association tethers a dimeric replicase containing both leading and lagging strand polymerases to the helicase, binding all components active in DNA replication together at the fork in one large replicosome assembly (18).

In the evolutionarily distant Gram-positive bacterium *B. subtilis*, conserved PriA proteins and the replicative helicase (termed DnaC in *B. subtilis*) participate in the replication restart primosome, but novel proteins, DnaD and DnaB, which are not homologs of *E. coli* primosomal proteins, intervene between PriA and association with the helicase/helicase loader. The *B. subtilis* helicase loader, DnaI, is also poorly conserved, so *B. subtilis* and other low GC Gram-positive bacteria may follow a novel pathway for primosome assembly. An ordered assembly mechanism (PriA-DnaD-DnaB-DnaI-DnaC) has been proposed (19). Another important difference between the *E. coli* and *B. subtilis* replication processes is that the proteins that act at intermediate stages between PriA and the helicase loader also participate in DnaA/origin-dependent initiation (20).

We have established a fully functional *B. subtilis* rolling circle replication system on mini-circular templates that recapitulate the known *in vivo* replication rate and the genetically defined protein requirements (21). This system allowed the function of two discrete Pol IIIs (DnaE and PolC) to be established. The PolC HE (PolC,  $\tau$ -complex, and  $\beta_2$ ) serves as the replicase for both the leading and lagging strands. Unlike in *E. coli*, the major replicase cannot efficiently elongate a primer provided by the DnaG primase. Instead, a protein functionally analogous to DNA polymerase  $\alpha$  in eukaryotes, DnaE, extends the RNA primer a short distance and hands off the product to the PolC HE.

Both the *E. coli* and *B. subtilis* rolling circle replication systems require an extensive preincubation in a reaction where the helicase is recruited and assembled before elongation is initiated. This is necessary to isolate the elongation events so they can be studied without the kinetic complications of a rate-limiting initiation. Thus, a well defined system amenable to convenient acquisition of kinetic data is needed to study PriA-dependent assembly of the restart primosome.

FRET assays have been developed using synthetic forks that permit monitoring helicase function (22, 23). In this report, we adapt this FRET assay and show that blocking the 5'-end of the lagging strand template sterically precludes self-assembly of the helicase and makes the reaction dependent on PriA and the other components of the replication restart primosome. We use this system to reveal that PriA specificity for replication fork structure is determined by the PriA ATPase. We also explore the mechanism by which PriA acts as a checkpoint protein, blocking the intrinsic strand displacement activity of the Pol III HE on incompletely assembled replication forks.

## EXPERIMENTAL PROCEDURES

**Oligonucleotides**—All oligonucleotides were obtained from Biosearch Technologies. Substrates used in all FRET experi-

ments and strand displacement reactions carried out in solution were assembled from the HPLC-purified oligonucleotides listed in Fig. 1E.

Substrates for fluorescent helicase assays and strand displacement reactions in solution were assembled by combining 1  $\mu$ M fluorescent leading strand template, 1  $\mu$ M quenching lagging strand template, and 1  $\mu$ M of the appropriate leading strand primer (or no primer) in a final volume of 25  $\mu$ l in a buffer containing 10 mM Tris-HCl (pH 7.75), 50 mM NaCl, and 1 mM EDTA. Samples were heated to 95 °C for 5 min and cooled to 25 °C, decreasing the temperature by 1 °C/min. Unprimed forked template was constructed from FT90 and QT90; 0-nucleotide (nt) gap forked template from FT90, QT90, and P0g; 2-nt gap forked template from FT90, QT90, and P2g; 5-nt gap forked template from FT90, QT90, and P5g; 10-nt gap forked template from FT90, QT90, and P10g; and 20-nt gap forked template from FT100, QT90, and P20g.

For experiments on streptavidin beads, a biotinylated 10-nt gap forked template was constructed from biotinylated primer 35-mer, 5'-TT(biotin)GAAGATTCTTACATTAGCCGACA-AAATCATATT-3' (biotin is conjugated to preceding modified thymidine); leading strand template 90-mer, 5'-CGC-GTATAGATCATTACTATAACATGTTAGATTTCATGATAATATACGAGATGACGAATATGATTTTGTCCGGCTAATGTAAGAATCTTCAA-3'; and lagging strand template 90-mer, 5'-TTATATTATCATGAATCTAACATGTTATAGTAATGATCTATACGCG-3'. Forked template was annealed identically to those for FRET experiments.

**Proteins**—*E. coli* Pol III HE and primosomal proteins were purified as described previously: Pol III (24),  $\epsilon$  (25),  $\tau$  (26),  $\delta$ ,  $\delta'$  (27),  $\chi$ ,  $\psi$  (28),  $\beta$  (29), single-stranded DNA binding protein (SSB) (30), and wild-type PriA, PriB, DnaT, DnaB, and DnaC (31). PriA K230R was a gift from Ken Marians (31). The  $\epsilon$  subunit used in our experiments was mutated at D12A and E14A to eliminate endogenous 3'-5'-exonuclease activity, which degrades the primer (32). *B. subtilis* protein components were purified as described for PolC, SSB,  $\beta$ ,  $\tau$ ,  $\delta$ , and  $\delta'$  (33) and DnaE, PriA, DnaD, DnaB, DnaC, and DnaI (21).

Streptavidin was obtained from New England BioLabs. In experiments using T7 polymerase, USB Sequenase (version 2.0) DNA Polymerase (Affymetrix) was used. This is a genetically modified variant consisting of two subunits: *E. coli* protein thioredoxin and genetically engineered bacteriophage T7 gene 5 protein where amino acids 118–145 are deleted to eliminate exonuclease activity. Polymerase activity is unaffected.

**FRET Helicase Assays**—Fluorescence helicase assays were carried out in a final volume of 50  $\mu$ l with 20 nM substrate and 100 nM trap oligonucleotide in a black, round-bottomed 96-well plate (from Greiner Bio-One, catalog no. 650209) in a buffer containing 50 mM HEPES (pH 7.5), 20% (v/v) glycerol, 0.02% (v/v) Nonidet P40 detergent, 200  $\mu$ g/ml BSA, 100 mM potassium glutamate, 10 mM DTT, 10 mM magnesium acetate, and 2 mM ATP. Unless otherwise noted, all substrates were preincubated for 5 min at room temperature with 200 nM streptavidin prior to the addition of other protein components. Helicase reactions were incubated at 30 °C for 15 min, which was within the linear time range of the assay under the condi-

tions reported. Fluorescence emission was read at 535 nm using an EnVision plate reader (PerkinElmer Life Sciences) with an excitation at 485 nm. The fluorescent plate reader was equipped with excitation filter FITC 485 and emission filter FITC 535. Unwound DNA concentration was related to fluorescence units using a linear calibration curve determined by fitting the fluorescence measurements of standard solutions with varying concentrations of unwound DNA. The standard solutions had concentrations ranging from 0 to 20 nM of unwound DNA in the reaction buffer with 100 nM trap oligonucleotide. The 0 nM point was taken to be when all of the fluorescent leading strand template was bound to the non-fluorescent quenching lagging strand template. The 20 nM standard was measured in the absence of quenching lagging strand template.

**PriA Blocking Strand Displacement Reactions**—The leading strand primer was labeled with  $^{32}\text{P}$  on the 5'-end using T4 polynucleotide kinase according to the manufacturer's instructions (Invitrogen) prior to annealing. Unincorporated [ $\gamma$ - $^{32}\text{P}$ ]ATP was removed using a Microspin-G25 spin column (GE Healthcare). Experiments were carried out in the same reaction buffer as FRET experiments.

For reactions carried out in solution, 20 nM substrate was added to protein components from the indicated source organism: 500 nM PriA, 500 nM SSB<sub>4</sub>, 500 nM  $\beta_2$ , 80 nM  $\tau_3$  complex, and 80 nM Pol III core (exo-) (or indicated *B. subtilis* polymerase) in a final reaction volume of 30  $\mu\text{l}$ . The samples were incubated for 5 min at room temperature. dNTPs were added to 100  $\mu\text{M}$  (final concentration) and incubated with the reaction for 5 min. The reactions were quenched in a sample of equal volume containing 96% formamide, 20 mM EDTA, and 1 mg/ml bromphenol blue, then heated to 95 °C for 4 min. The samples were resolved by denaturing electrophoresis at 10 watts for 2 h in a 12% polyacrylamide gel (19:1 acrylamide:bisacrylamide) containing 8 M urea using 100 mM Tris borate and 2 mM EDTA as electrophoresis running buffer. Gels were dried onto DEAE paper and scanned by a phosphorimaging device.

For reactions carried out on streptavidin beads, 600 fmol of radiolabeled, biotinylated primer/10-nt gap forked template were bound to 25  $\mu\text{l}$  of streptavidin beads (Promega Tetralink Tetrameric Avidin) pre-equilibrated in the reaction buffer. The forked template was incubated with the beads for 10 min at room temperature. The beads were then washed three times with 200  $\mu\text{l}$  of reaction buffer to remove any unbound substrate. The bead-bound substrate was then incubated with 500 nM PriA, 500 nM SSB<sub>4</sub>, 500 nM  $\beta_2$ , 80 nM  $\tau_3$  complex, and 80 nM Pol III core (exo-) at room temperature for 15 min. The beads were then washed five times with 200  $\mu\text{l}$  of the reaction buffer to remove free protein. dNTPs and/or primosomal proteins (PriB, DnaT, DnaB, and DnaC) were added to the reaction and incubated at room temperature for 15 min. The helicase loading conditions were independently optimized for this assay: 50 nM PriB<sub>2</sub>, 500 nM DnaT<sub>3</sub>, 12 nM DnaB<sub>6</sub>, and 25 nM DnaC (supplemental Fig. S4). The reaction was quenched with 100 mM EDTA and 2% SDS. The product was removed from the bead by incubating with 20  $\mu\text{g}$  of proteinase K at 37 °C for 1 h. A portion of the supernatant was then added to an equal volume of buffer containing 100 mM Tris borate, 2 mM EDTA, 20% (v/v) glycerol,

1 mg/ml bromphenol blue, and 1 mg/ml xylene cyanol FF prior to resolving in a native gel to assay helicase activity. These samples were resolved by electrophoresis at 75 V for 18 h in a 12% polyacrylamide gel (37.5:1 acrylamide:bisacrylamide) using the same electrophoresis buffer as denaturing gels. The gel was dried and scanned by a PhosphorImager. A separate portion of the supernatant was analyzed by denaturing PAGE.

## RESULTS

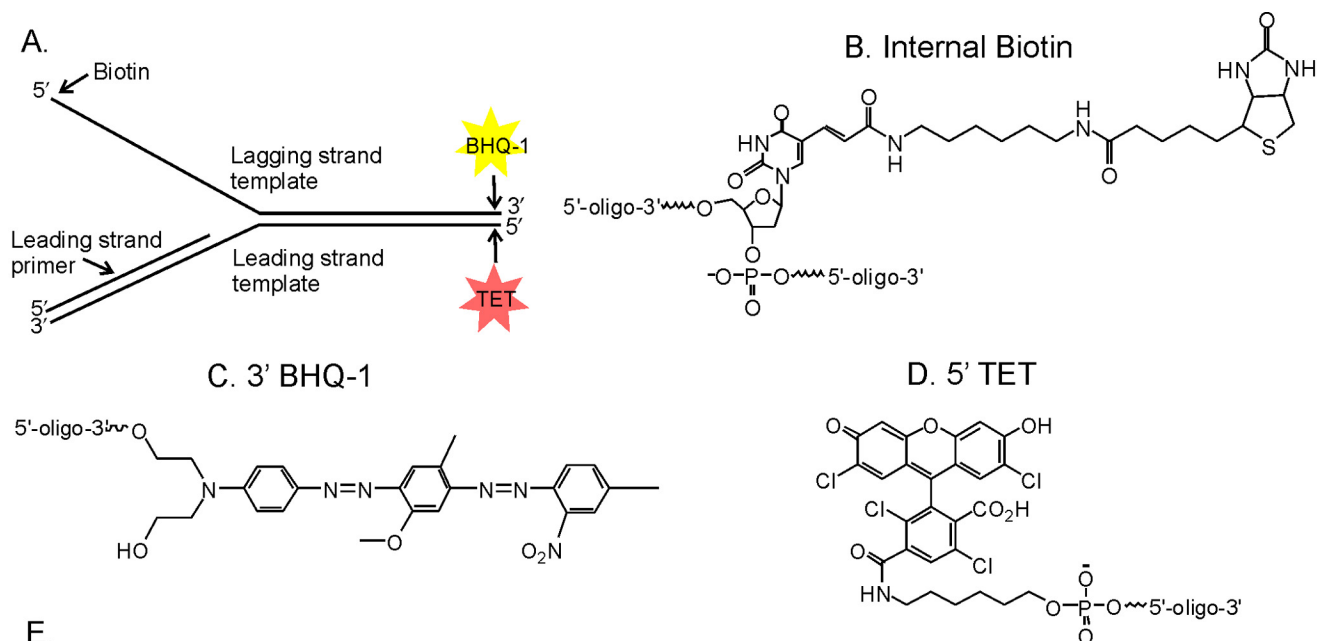
**Development of a FRET Assay for Primosome Function**—We adapted a FRET-based assay for helicase function (22) and optimized it for studying the helicase loading apparatus from two representative Gram-negative and Gram-positive organisms, *E. coli* and *B. subtilis*. The system employed model replication forks constructed from synthetic oligonucleotides with a fluorophore opposed by a quencher in the opposing strand (Fig. 1). Splitting the two strands apart results in an increase in fluorescence. We used an excess of a trapping oligonucleotide that was complementary to the duplex region of the leading strand template to sequester strands split apart by helicase so that they do not reanneal. The leading strand template contained an annealed primer that modeled the leading strand replication product. Primers were synthesized with a variable sized gap between their 3'-ends and the fork. The 5'-end of the lagging strand also contained a biotin to which streptavidin could be bound, providing a steric block.

Titration of high concentrations of either the *E. coli* DnaB helicase or the *B. subtilis* DnaC replicative helicase onto templates in the absence of other proteins allowed helicase self-loading and function leading to extensive unwinding (Fig. 2A). To determine whether the hexameric helicase self-assembles on DNA by a mechanism where it threads over a free 5'-end, we blocked the 5'-end of model substrates with streptavidin (Fig. 1). When the 5'-end of the lagging strand template at the fork was blocked, neither *E. coli* nor *B. subtilis* helicases were able to self-assemble (Fig. 2B). In the absence of streptavidin, the cognate SSB also prevents helicase self-loading in both systems (Fig. 2C).

To establish an optimal system for helicase loading that is dependent upon *E. coli* and *B. subtilis* primosomal proteins, we blocked the single-stranded 5'-end of forked templates with streptavidin to eliminate the helicase self-loading background and titrated each component to determine its optimum concentration (Fig. 3 and 4). The optimal level was selected for subsequent experiments except for SSB. We selected an excess, slightly inhibitory level, which proved effective in blocking helicase self-loading (Fig. 2C).

The preceding experiment was conducted under conditions using a forked substrate containing a 10-nt gap between the leading strand 3'-primer terminus and the fork. Similar experiments were conducted with a substrate that contained no gap (supplemental Figs. S1 and S2). Similar results were obtained, except higher concentrations of PriA, PriB, DnaT, and DnaC were required in the *E. coli* system and higher levels of PriA, DnaB, DnaD, and DnaI were required in the *B. subtilis* system. Thus, both systems required higher levels of all proteins that act prior to helicase loading, suggesting a lower functional affinity for templates that do not contain a gap in the leading strand.

## PriA Specificity and Function



### Fluorescent Leading Strand Template 90-mer (FT90)

5'-TET-CGCGTATAGATCATTACTATAACATGTTAGATTCATGATAATATACGAGATGACGAATATGATTTTGTCGGCTAATGTAAGAATCTTCAA-3'

### Quenching Lagging Strand Template 90-mer (QT90)

5'-TT(biotin)TTTATATTATCATGAATCTAACATGTTATAGTAATGATCTATACGCG-BHQ-1-3'

### Fluorescent Leading Strand Template 100-mer (FT100)

5'-TET-CGCGTATAGATCATTACTATAACATGTTAGATTCATGATAATATACGAGATGACGAATATGATTTTGTCGGCTAATGTAAGAATCTTCAAATGATCGTAG-3'

### 0 Nucleotide Gap Leading Strand Primer (P0g)

5'-TTGAAGATTCCTACATTAGCCGACAAAATCATATTCGTCATCTCG-3'

### 2 Nucleotide Gap Leading Strand Primer (P2g)

5'-TTGAAGATTCCTACATTAGCCGACAAAATCATATTCGTCATCT-3'

### 5 Nucleotide Gap Leading Strand Primer (P5g)

5'-TTGAAGATTCCTACATTAGCCGACAAAATCATATTCGTC-3'

### 10 Nucleotide Gap Leading Strand Primer (P10g)

5'-TTGAAGATTCCTACATTAGCCGACAAAATCATATT-3'

### 20 Nucleotide Gap Leading Strand Primer (P20g)

5'-CTACGATCATTGAAGATTCCTACATTAGCCGACA-3'

### Trap Oligonucleotide

5'-TATATTATCATGAATCTAACATGTTATAGTAATGATCTATACGCG-3'

**FIGURE 1. Model replication fork and oligonucleotides used in FRET helicase assays.** *A*, DNA substrate used in FRET unwinding reactions. Fluorescence of tetrachloro fluorescein (*TET*) on the 5' terminus of the leading strand increases when separated from black hole quencher 1 (*BHQ-1*) on the lagging strand. *B*, internal biotin conjugated to modified thymidine. *C*, black hole quencher 1 conjugated to 3'-end of the lagging strand. *D*, tetrachloro fluorescein conjugated to 5'-end of the leading strand. *E*, sequences of oligonucleotides (*oligo*) used to build substrates depicted in *A* for FRET assays. T(biotin) indicates the internal biotin modification in *B*.

Our initial forked substrate contained 90-nt leading and lagging strand templates with a 45-nt duplex ahead of the fork. This represented close to the longest practical length considering economic factors and current commercial capabilities for producing substituted oligonucleotides. Systematic efforts to decrease the size resulted in decreased activities (supplemental Table S1). Thus, we retained the use of forks composed of annealed 90-mers for most experiments.

*The Intrinsic PriA ATPase Is Required for Primosome Assembly on Forks Containing Leading Strand Gaps*—The preference for forked templates with variable gap length was determined. We observed significantly higher function with templates with the largest (10-nt) gap size in both the *E. coli* and *B. subtilis*

primosomal systems (Fig. 5, *A* and *D*). In an earlier study, the opposite result was observed using a PriA derivative in which the intrinsic ATPase required to drive a 3'→5' helicase activity was inactivated (11, 34). To permit a direct comparison, Ken Marians kindly provided some of the PriA K230R used in that study. Using our FRET assay, we reproduced their results (Fig. 5*B*). Thus, the reversal in gap size preference and the ability to efficiently use templates with gaps requires the activity of the PriA ATP-dependent helicase (Fig. 5*C*). The results reported in Fig. 5 were obtained under conditions optimized for forked templates containing a 10-nt gap. To ensure that the result was not condition-specific, we repeated the experiment using conditions that had been optimized for templates lacking a gap

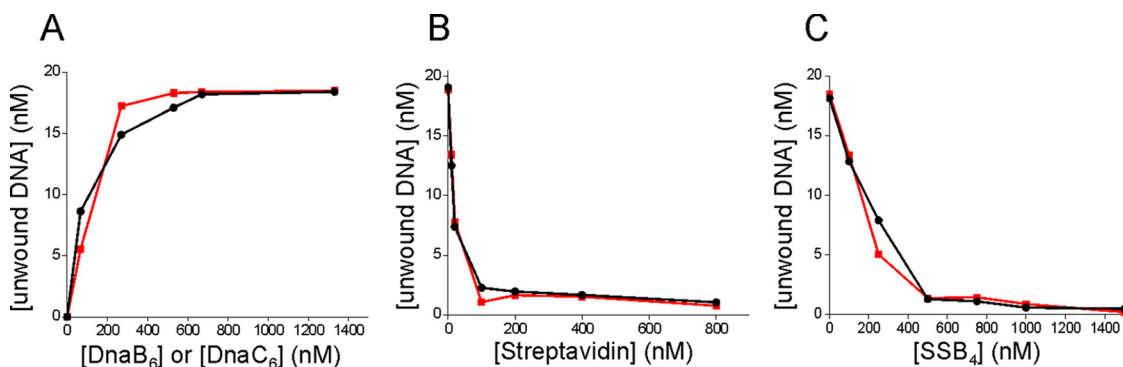


FIGURE 2. *E. coli* and *B. subtilis* helicases self-load onto replication forks by threading onto a free 5'-end on the lagging strand. Titrations performed against 20 nM unprimed forked template in the absence of streptavidin unless stated otherwise. A, 550 nM *E. coli* DnaB<sub>6</sub> (red) and *B. subtilis* DnaC<sub>6</sub> (black). B, streptavidin inhibits helicases from self-loading onto replication forks by binding to a biotin near the 5'-end of the lagging strand. Streptavidin was titrated using *E. coli* DnaB<sub>6</sub> (red) or *B. subtilis* DnaC<sub>6</sub> (black). C, SSB can block the 5'-end of the lagging strand and prevent helicases from self-loading. *E. coli* or *B. subtilis* SSB was titrated in the presence of *E. coli* DnaB<sub>6</sub> (red) or *B. subtilis* DnaC<sub>6</sub> (black), respectively.

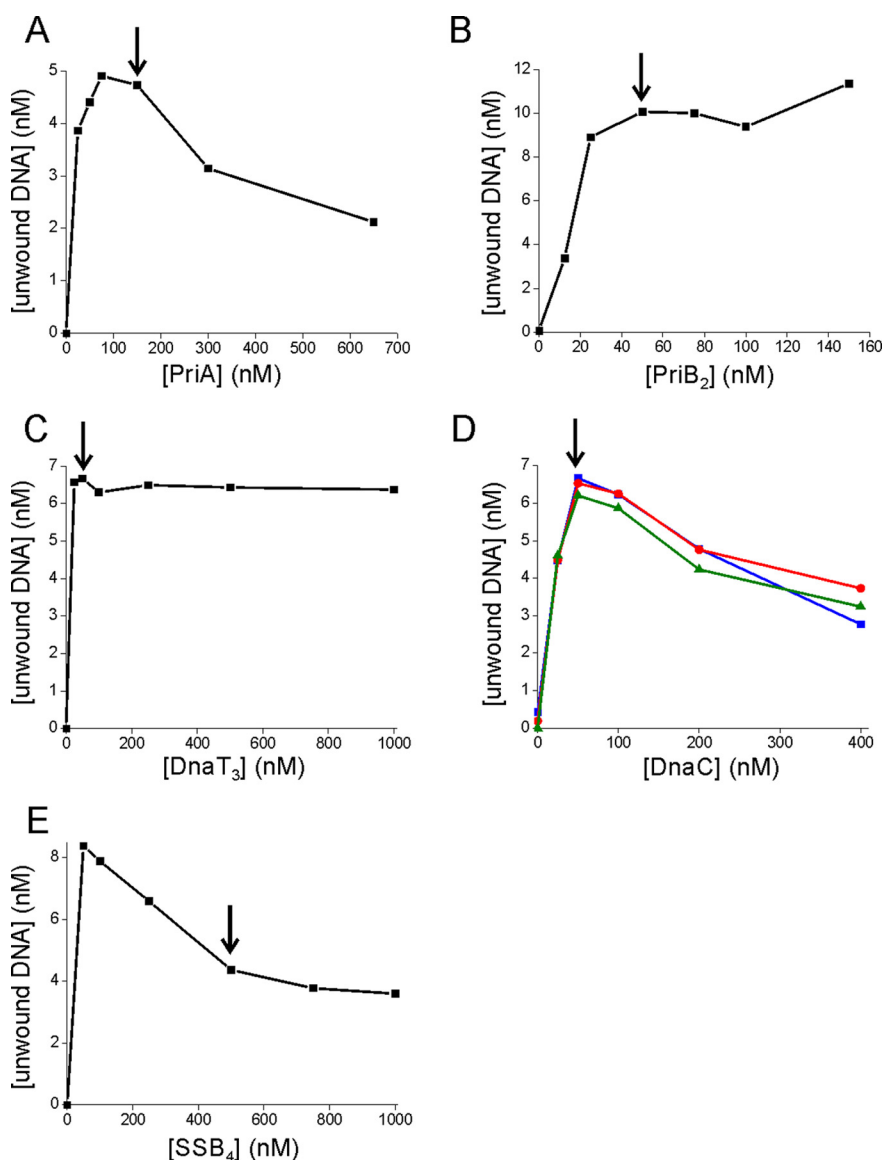
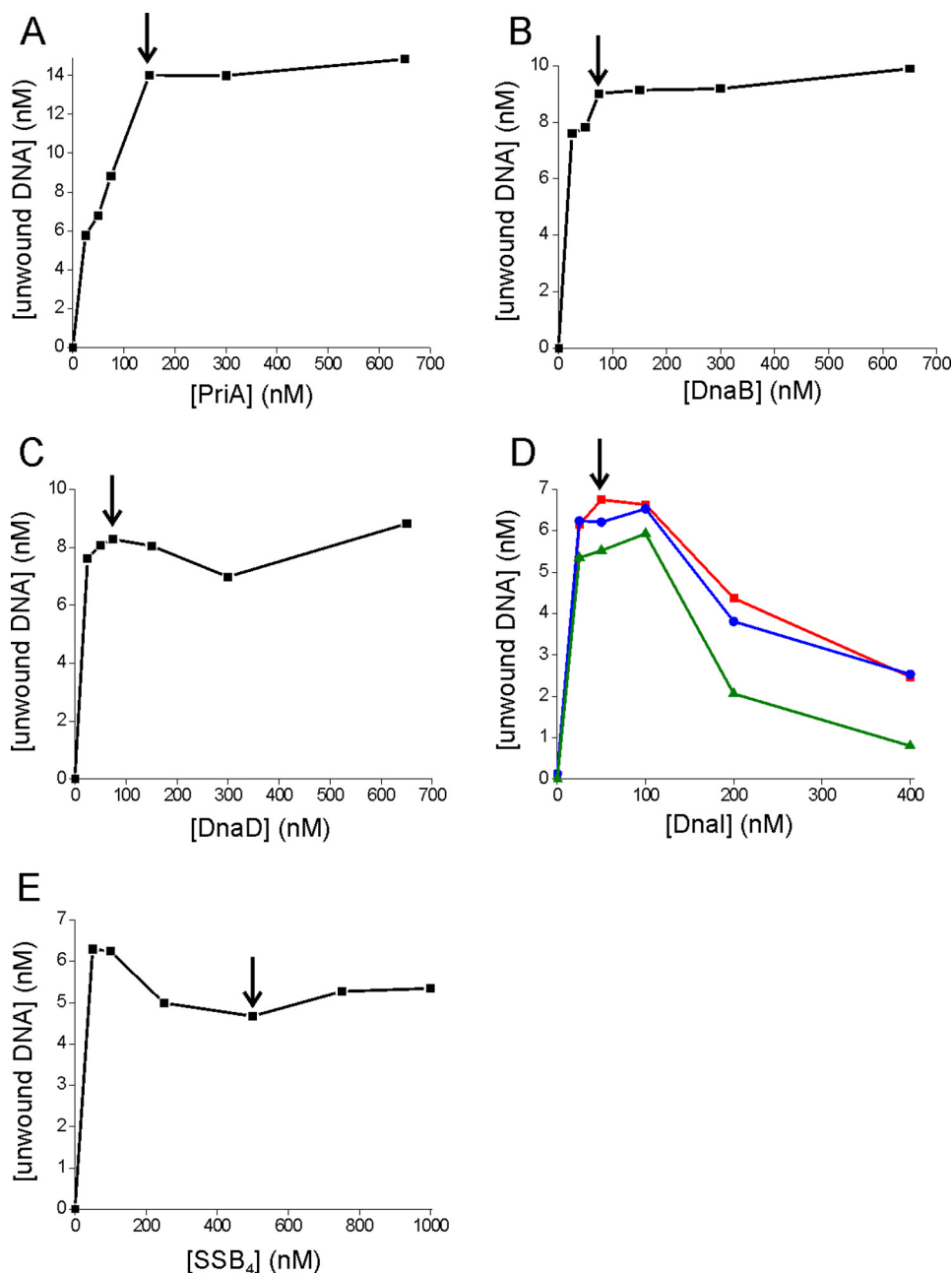


FIGURE 3. Optimizing *E. coli* protein concentrations using the 10-nt gap forked template. Helicase loading proteins and helicase were titrated sequentially (in the order they appear here) in the presence of all other primosomal proteins; the arrow indicates the chosen optimum for each. In subsequent experiments, that optimal level was used. The starting conditions used were as follows: 75 nM PriB<sub>2</sub>, 250 nM DnaT<sub>3</sub>, 12 nM DnaB<sub>6</sub>, 100 nM DnaC, and 500 nM SSB<sub>4</sub>. The final optimized conditions from this series of experiments were as follows: 150 nM PriA, 50 nM PriB<sub>2</sub>, 50 nM DnaT<sub>3</sub>, 12 nM DnaB<sub>6</sub>, 50 nM DnaC, and 500 nM SSB<sub>4</sub>. A, PriA titration; B, PriB<sub>2</sub> titration; C, DnaT<sub>3</sub> titration; D, DnaC helicase loader titrated at three different DnaB<sub>6</sub> concentrations (6 nM (green), 12 nM (red), and 24 nM (blue)); E, SSB<sub>4</sub> titration. To prevent the helicase self-loading reaction, 500 nM SSB<sub>4</sub> was used for further experiments.

## PriA Specificity and Function



**FIGURE 4. Optimizing *B. subtilis* protein concentrations on 10-nt gap forked template.** The experiment was carried out as described in the legend to Fig. 3. The starting conditions used were as follows: 300 nM DnaB, 300 nM DnaD, 12 nM DnaC<sub>6</sub>, 200 nM DnaI, and 500 nM SSB<sub>4</sub>. The final optimized conditions from this series of experiments were as follows: 150 nM PriA, 75 nM DnaB, 75 nM DnaD, 12 nM DnaC<sub>6</sub>, 50 nM DnaI, and 500 nM SSB<sub>4</sub>. A, PriA titration; B, DnaB titration; C, DnaD titration; D, DnaI helicase loader titrated at three different DnaC<sub>6</sub> helicase concentrations (6 nM (green), 12 nM (red), and 24 nM (blue)); E, SSB<sub>4</sub> titration. To prevent the helicase self-loading reaction, 500 nM SSB<sub>4</sub> was chosen for further experiments.

between the fork and the leading strand and obtained the same result (supplemental Fig. S3).

**PriA Functions as a Checkpoint Protein by Binding to Forks and Blocking Pol III HE Binding to the 3' Terminus of the Leading Strand**—In addition to PriA serving as the lead protein in directing primosomal assembly and replicative helicase loading, it functions as a checkpoint protein, at least in *E. coli*, blocking the intrinsic strand displacement activity of the Pol III HE on forks lacking the replicative helicase (12, 13). We confirmed this result, using our FRET assay template with radiolabeled primers, permitting assay for primer extension, on templates containing 2- and 20-nt gaps (Fig. 6A, lanes 3 and 6). We

observed, however, that we needed to add PriA before we added SSB. If we added SSB first, the checkpoint activity of PriA was not observed (compare Fig. 6A, lanes 2 with 3 and lanes 5 with 6). We also observed that the action of PriA in blocking the progression of Pol III is dependent upon a forked structure. Omitting the lagging strand template from the reaction does not support PriA functioning as a checkpoint protein (Fig. 6A, lanes 9 and 11). A control used to validate the assay (lane 8) shows that SSB is required to support strand displacement (13).

Next, we sought to determine whether *B. subtilis* PriA blocked the *B. subtilis* polymerases PolC HE and DnaE HE. As in the *E. coli* system, *B. subtilis* PriA served as a checkpoint

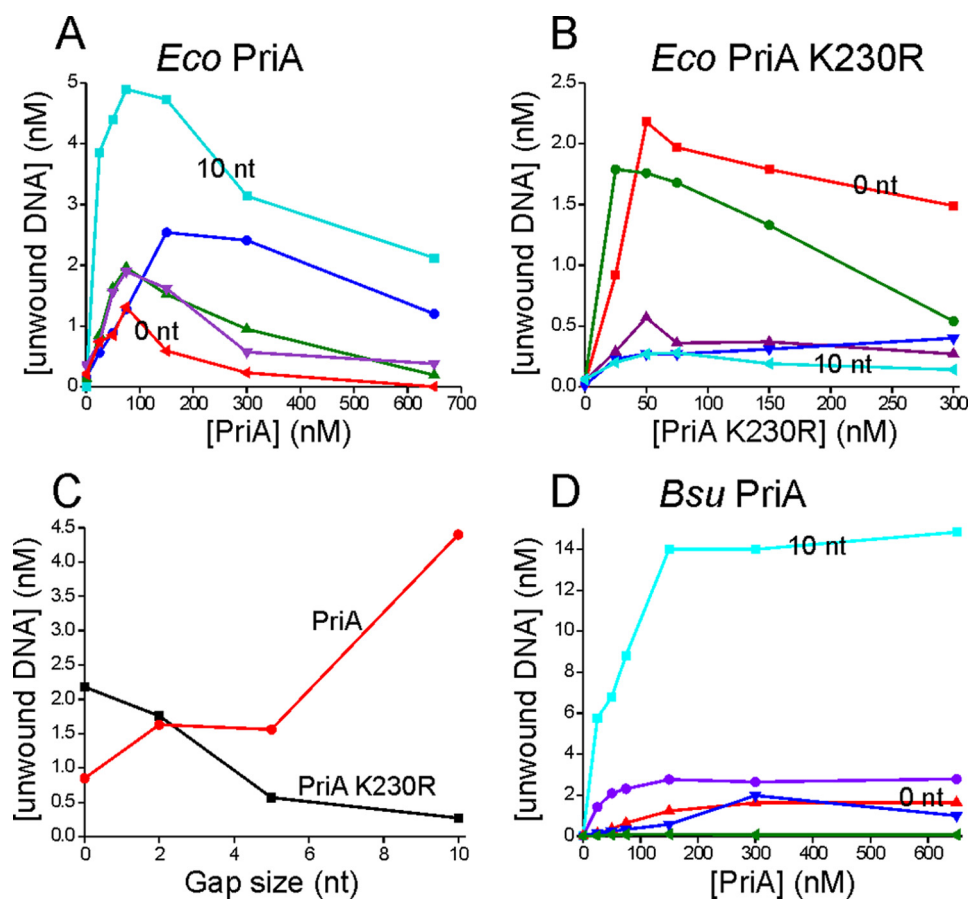


FIGURE 5. **Wild-type PriA containing a functional ATPase prefers forked substrates with large leading strand gaps.** For A, B, and D, five substrates were used: unprimed forked template (blue), 0-nt gap forked template (red), 2-nt gap forked template (green), 5-nt gap forked template (purple), or 10-nt gap forked template (cyan). Optimal *E. coli* protein concentrations listed in the legend of Fig. 3 were used. A, wild-type PriA (*E. coli*) titration; B, PriA K230R (*E. coli*) titration; C, amount of DNA unwound plotted against gap size at 50 nM wild-type PriA (red) and 50 nM PriA K230R (black) for *E. coli*; D, *B. subtilis* PriA titration. Optimal *B. subtilis* protein concentrations listed in the legend of Fig. 4.

protein that blocked the forward progression of both polymerases, but only if added before SSB (Fig. 6, B and C).

We next sought to determine whether the reaction was specific for cognate polymerases. We observed that both the PriAs could block *E. coli* Pol III HE and *B. subtilis* Pol C and DnaE HES with equal efficiency. Furthermore, *B. subtilis* PriA blocked a polymerase that is not homologous to Pol IIIs, T7 DNA polymerase, completely. The *E. coli* PriA inhibited T7 significantly with only a small portion of the product reaching full length (Fig. 6D). The experiment shown was conducted with a template containing a 2-nt leading strand gap. Essentially, the same result was obtained on templates containing a 20-nt gap (data not shown).

Two models exist for PriA function. When the checkpoint action of the PriA protein was initially discovered, it was suggested that PriA may just act as a steric block, denying access of the Pol III HE to the primer terminus (12). Later, a multifunction protein from bacteriophage T4, gp59, that is not homologous to PriA but exhibits similar checkpoint activity, was shown to function by binding to the blocked T4 polymerase at forks, forming an inactive ternary complex (35) until the helicase is loaded, which releases the inhibition. We chose to distinguish these two models, using *E. coli* PriA and Pol III HE. A system was developed where the forked template was immobilized on

streptavidin beads, allowing rapid washing and determination of the proteins bound functionally (Fig. 7A). The Pol III HE once bound to DNA in an initiation complex requires bumpers to prevent it from sliding off. Thus, we moved the biotin from the lagging strand template to the 5'-end of the leading strand primer. The fork functioned as a bumper on the other end of the primer. The presence of SSB served to prevent self-assembly of helicase.

In the absence of primosomal proteins, the Pol III HE could efficiently form initiation complexes on primed bead-bound replication forks that survived washing and extensively elongated the leading strand primer in a strand displacement reaction upon addition of dNTPs (Fig. 7B, lane 3). The observed reaction was dependent upon the presence of  $\beta_2$ , indicating it proceeds from authentic initiation complexes rather than residual polymerase not removed by the washing step (Fig. 7B, lane 8). Elongation did not occur in the absence of SSB, a required cofactor for the strand displacement activity of Pol III HE (Fig. 7B, lane 9) (13).

Addition of PriA to the reaction in the absence of other primosomal proteins prevented extension of primers, either by blocking Pol III HE binding or arresting the polymerase in an inactive state (Fig. 7B, lane 4). The remaining primosomal proteins were added to permit PriA-directed helicase assembly,

## PriA Specificity and Function

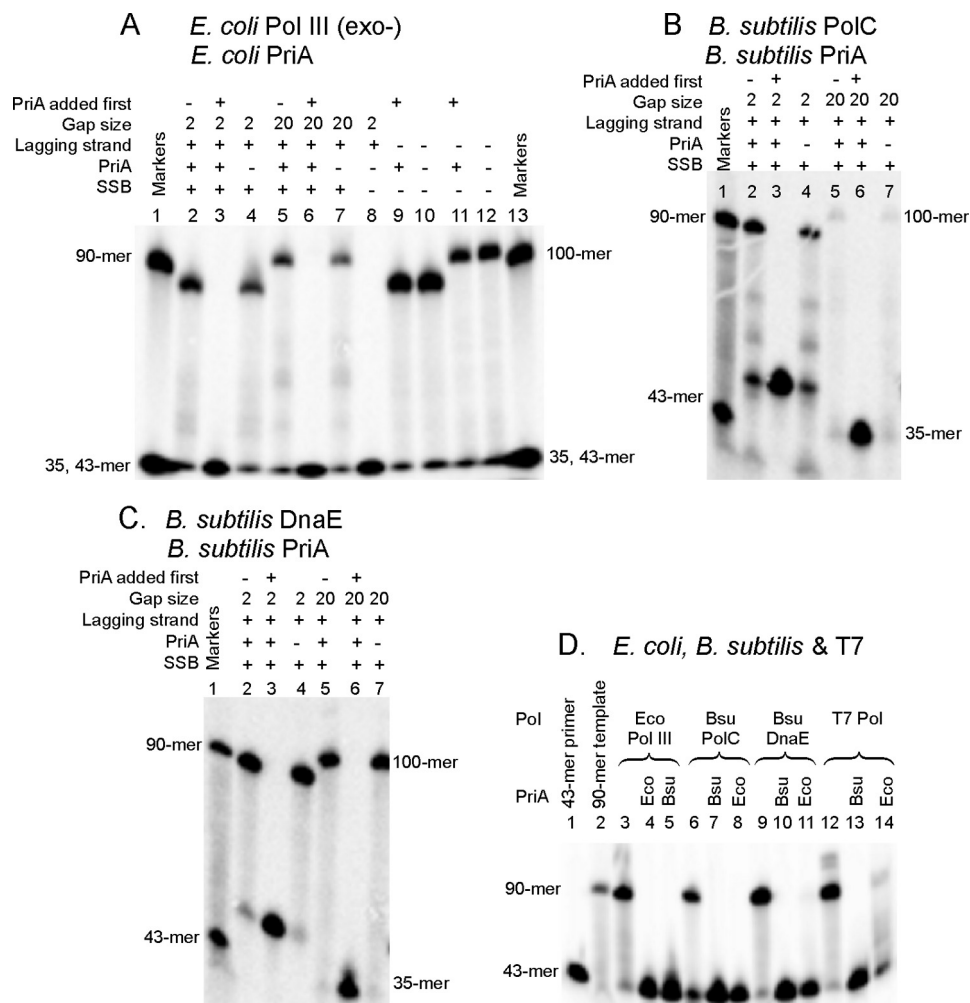


**FIGURE 6. PriA blocks the strand displacement reaction by Pol III HE in *E. coli* and by both *B. subtilis* Pol IIIs.** <sup>32</sup>P-labeled products of strand displacement were resolved in 12% polyacrylamide with 8 M urea. Substrates are either a 2-nt gap forked template (giving a 90-mer product) or a 20-nt gap forked template (giving a 100-mer product). Substrates without a lagging strand consist of just primer bound to leading strand template. In reactions where PriA was not added first (lanes 2 and 5 in A–C) but is present in the reaction, PriA was added immediately after SSB, but before HE. A, *E. coli* Pol III (exo-) HE and *E. coli* PriA. Lanes 9–12 contain a substrate composed of only primed template. Substrates in lanes 9 and 10 are constructed from FT90 and P2g and lanes 11 and 12 from FT100 and P20g. B, *B. subtilis* PolC HE and *B. subtilis* PriA. C, *B. subtilis* DnaE HE and *B. subtilis* PriA. D, PriA blocks the strand displacement reaction across species. All reactions were carried out on 20 nm 2-nt gap forked template. Reactions with *E. coli* Pol III HE and with T7 polymerase were performed with exonuclease-deficient polymerase. Lanes 1 and 2 contain markers to indicate the migration of the primer (43-mer) and the expected product (90-mer).

yielding an active helicase. Control reactions run on native gels detect a labeled primed leading strand (35/90) split from the lagging strand template permitting an independent assessment of helicase function (Fig. 7C). These control experiments indicated that 40% of the bead-bound forks contained an active helicase (Fig. 7C, lane 7). Yet, no elongation product was observed in the corresponding lane 7 in Fig. 7B. If Pol III HE was present, sequestered in an inactive complex with PriA, elongation would have been expected at a 40% of the level we observed in lane 3 once helicase was loaded, relieving inhibition by PriA. We could have detected elongation at a level of 1%, judging by the control shown in Fig. 7B, lane 13. Another control reaction where the washing step was omitted confirmed that PriA inhibition of the Pol III HE is relieved on the bead-bound substrate upon helicase assembly (Fig. 7D).

To check whether the result observed was caused by the 10-nt gap, being too small to accommodate both Pol III HE and PriA at a fork, we repeated the experiment reported in Fig. 7 using a substrate containing a 20-nt gap and observe the same

result (supplemental Fig. S5). We conclude that PriA acts as a checkpoint protein by blocking Pol III HE binding.

## DISCUSSION

In this work, we have used synthetic model replication forks to study aspects of the replication restart reaction in divergent Gram-negative and Gram-positive model organisms. It has been estimated that *E. coli* and *B. subtilis* diverged approximately two billion years ago, a greater evolutionary distance than yeast and humans (Ref. 36 and references therein). Important differences have been observed in the replication systems of *E. coli* and *B. subtilis* that suggest that the extensive replication studies conducted with *E. coli* do not always present an accurate model for replication in all bacteria (37). For example, *B. subtilis* requires two DNA polymerase IIIs for replication, whereas *E. coli* requires only one (38). It has been demonstrated that the second Pol III (DnaE) has a specialized role in lagging strand primer processing analogous to the role of DNA polymerase  $\alpha$  in eukaryotes (21). Additional proteins participate in

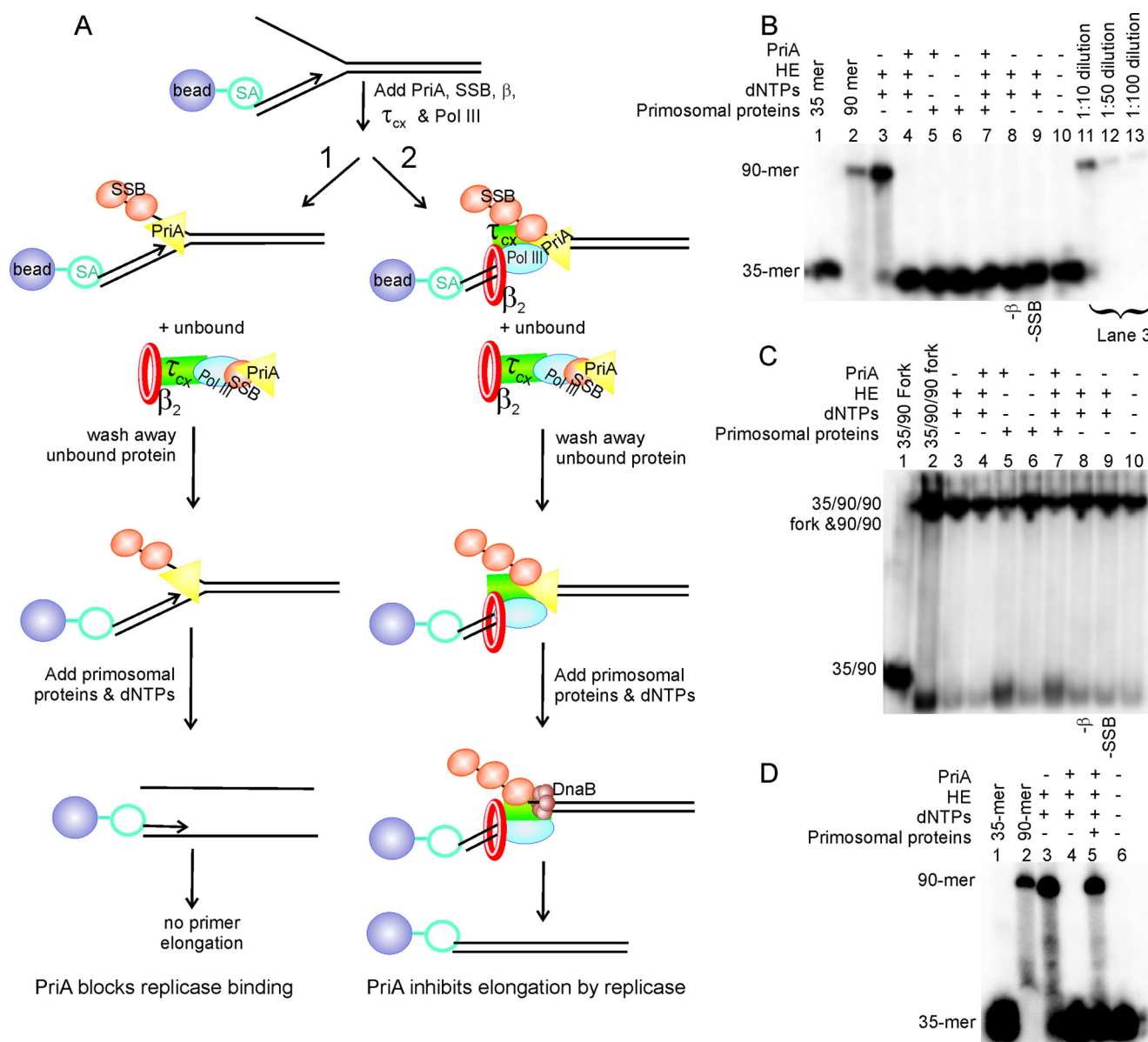


**FIGURE 7. PriA and holoenzyme do not coexist on PriA-inhibited replication forks.** *A*, diagram depicting two possible models of PriA inhibiting the strand displacement reaction and the expected result for each reaction on streptavidin (SA) beads. The primer is labeled on the 5'-end with  $^{32}\text{P}$  so that primer extension and helicase activity can be monitored. The primer contains a biotin near the 5'-end so that substrates can be conjugated to streptavidin-linked beads. *Scheme 1* depicts PriA blocking the 3'-OH of the primer, physically preventing Pol III HE from binding. *Scheme 2* portrays an inhibition model where both PriA and Pol III HE bind to the substrate. Primosomal proteins (PriB, DnaT, DnaB, and DnaC) were added as described under "Experimental Procedures." *B*, denaturing gel analysis to monitor primer extension by *E. coli* Pol III (exo-). *Lanes 1–3* are dilutions of the positive control *lane 3* to establish detection limits. For both *B* and *C*, *lanes 8 and 9* contain the full Pol III HE but in *lane 8*, the  $\beta$ -subunit was omitted, and in *lane 9*, SSB was omitted. *C*, native gel analysis to monitor substrate unwinding by *E. coli* DnaB helicase. The *upper band* is the replication fork, and the 90/90 duplex product in those cases is where replication occurs. The *lower band* is the displaced leading strand primer template. In *lane 5*, ~45% of the substrate was unwound by the helicase. In *lane 7*, ~40% of the substrate was unwound by the helicase. In all other lanes, the amount of substrate unwound is not significantly above background. *D*, denaturing gel analysis to monitor primer extension by *E. coli* Pol III (exo-) on immobilized substrate without a washing step. Experiment carried out as described under "Experimental Procedures," except after incubation with Pol III HE components, the washing steps were omitted. In *lane 5*, ~45% of the primer is elongated.

initiation reactions, both at the origin and at the restart replication fork, that have no homologs in *E. coli* (39). Thus, having a Gram-positive system to compare with *E. coli* will permit further understanding of the mechanistic basis for their functional divergence.

We adapted a simple FRET assay that has been used in the study of other helicases (22). By blocking the 5'-end of the lagging strand, we were able to make both the *E. coli* and *B. subtilis* systems dependent on PriA and the remaining primosomal proteins. This indicates that the replicative heli-

case self-assembly reactions proceed by threading of pre-assembled hexamers over free 5'-ends of model forks. An example of the alternative model, where a hexameric helicase could transiently open and close, sequestering a single-stranded template, has been provided by the double-stranded RNA virus  $\Phi 12$  helicase (40). This latter type of assembly should not be inhibited by a steric block on the 5'-end of the lagging strand template. The helicase self-assembly reaction only takes place at very high, non-physiological concentrations of helicase. We can conclude that this

## PriA Specificity and Function

does not represent a common pathway *in vitro* consistent with genetic evidence that it does not take place *in vivo* (41, 42).

Our initial forked substrate contained 90-nt single-stranded leading and lagging strand templates with a 45-nt duplex ahead of the fork. Systematic efforts to decrease their size resulted in significantly decreased activity. This result contrasts markedly from the requirements of model forks for reactions that only contain replicative helicase in self-assembly reactions (43). There, a 15-nt lagging strand arm is sufficient to support an efficient reaction and a 10-nt arm is adequate for the reaction, although a 5-nt arm is not. In our system, a 15-nt lagging strand arm is inert (supplemental Table S1). Because it is thought that only the first 6–10 nts of the lagging strand tail productively interact with the helicase, the remaining length requirement must be for additional protein factors to bind. At least part of the binding site for PriA, PriB and DnaT is near the fork (14), but these factors productively interact with SSB (44, 45), and additional lagging strand length is likely required to accommodate that interaction. The requirement for a long duplex ahead of the fork and within the leading strand arm is less explicable. Future studies, perhaps led by DNA site-specific cross-linking will likely provide insight into which factors interact within these regions.

We also examined the effect of the size of the gap between the 3'-end of the leading strand and the fork. We found differences depending on whether the ATPase within the PriA protein was active. PriA K230R with an inactive ATPase exhibits a strong preference for substrates with small or no gaps. Templates with gaps of 10-nt are inactive, consistent with published observations (34). However, with ATPase-proficient wild-type PriA, the result is just the opposite, with discrimination against substrates with short gaps and the highest activity on substrates with 10-nt gaps. To our knowledge, this observation is without precedent. Although a large number of nucleic acid transactions are driven by ATPases and a large number of reactions are activated or dissociated by ATPase activity, we know of none where specificity in two robust reactions is reversed by the presence of an ancillary ATPase.

In addition to its key role in initiating primosome assembly, PriA serves as a checkpoint protein that prevents Pol III HE from catalyzing a strand displacement reaction in the absence of a replicative helicase at the fork (12). One model initially proposed was that PriA merely blocked access of the Pol III HE to replication forks. Another model was provided by the established mechanism of phage T4 gp59. Gp59 serves as a helicase loader and also as a checkpoint protein. Although not homologous, its function is analogous to PriA. Gp59 binds to forks and the T4 DNA polymerase, locking it into an inactive conformation in a stable ternary complex (35). Using forked templates bound to beads allowed rapid washing after complex formation so that bound components could be determined. We showed that PriA excluded Pol III HE, as initially hypothesized. Control experiments showed that in the absence of PriA, Pol III HE could form initiation complexes on primed forked templates.

Further supporting a nonspecific steric role for PriA in blocking strand displacement is our observation that PriA can block non-cognate polymerases. *E. coli* PriA can block strand dis-

placement catalyzed by the *B. subtilis* Pol C and DnaE HEs, and *B. subtilis* PriA blocks strand displacement by the *E. coli* Pol III HE. It is conceivable that conserved protein interaction sites could enable the inhibition observed. But, we also demonstrated that both the *B. subtilis* and *E. coli* PriA proteins could block T7 DNA polymerase, which is not homologous to DNA Pol IIIs. These experiments also establish a checkpoint role for *B. subtilis* PriA, showing the original *E. coli* observation (12) is general.

In all assays conducted for this study, we observed that PriA had to be added before SSB for it to display function. Presumably, if added first, SSB covers the PriA binding site and prevents its interaction with the fork. However, in dynamic reactions where Pol III HE is catalyzing a strand displacement reaction that is dependent upon its interaction with SSB on the lagging strand, addition of PriA immediately stops the reaction (13). This could be explained if PriA can bind to an initial segment of single-stranded DNA exposed on the lagging strand of the fork that is too small to stably or rapidly bind SSB. In this reaction, there could be transient interactions with Pol III HE, facilitating its displacement, but our results show a stable complex is not formed.

The substrates, assays, and basic principles established by this study provide a foundation for further pursuit of the mechanistic basis of differences between the replication restart reaction in Gram-negative and low GC Gram-positive bacteria. The simple oligonucleotide substrates should be amenable to cross-linking studies, using nucleotide position-specific modifications, kinetic studies, screens for small molecule inhibitors, and structural studies.

---

*Acknowledgments*—We thank Ken Mariani for providing overproducing strains for all of the primosomal proteins and for advice on purification and establishing rolling circle reactions. We also thank Ken Mariani for providing PriA K230R that allowed us to confirm initial observations, providing a critical control for showing the ATPase of PriA shifts the specificity of this protein toward substrates with large gaps. We thank Diane Hager for preparation of figures and Melissa Stauffer of Scientific Editing Solutions for editing the manuscript. We also thank Quan Yuan for providing *E. coli* primosomal proteins and advice on use, Garry Dallmann for advice on setting up the FRET assay and Paul Dohrmann for working out procedures for isolation of initiation complexes on templates bound to streptavidin beads.

---

## REFERENCES

1. Kaguni, J. M. (2006) DnaA: controlling the initiation of bacterial DNA replication and more. *Annu. Rev. Microbiol.* **60**, 351–375
2. Mott, M. L., and Berger, J. M. (2007) DNA replication initiation: mechanisms and regulation in bacteria. *Nat. Rev. Microbiol.* **5**, 343–354
3. Cox, M. M., Goodman, M. F., Kreuzer, K. N., Sherratt, D. J., Sandler, S. J., and Mariani, K. J. (2000) The importance of repairing stalled replication forks. *Nature* **404**, 37–41
4. Mariani, K. J. (2000) PriA-directed replication fork restart in *Escherichia coli*. *Trends Biochem. Sci.* **25**, 185–189
5. Polard, P., Marsin, S., McGovern, S., Velten, M., Wigley, D. B., Ehrlich, S. D., and Brund, C. (2002) Restart of DNA replication in Gram-positive bacteria: functional characterisation of the *Bacillus subtilis* PriA initiator. *Nucleic Acids Res.* **30**, 1593–1605
6. Ng, J. Y., and Mariani, K. J. (1996) The ordered assembly of the  $\phi$ -X174-

- type primosome: I isolation and identification of intermediate protein-DNA complexes. *J. Biol. Chem.* **271**, 15642–15648
7. McGlynn, P., Al-Deib, A. A., Liu, J., Mariani, K. J., and Lloyd, R. G. (1997) The DNA replication protein PriA and the recombination protein Recg bind D-loops. *J. Mol. Biol.* **270**, 212–221
  8. Nurse, P., Liu, J., and Mariani, K. J. (1999) Two modes of PriA binding to DNA. *J. Biol. Chem.* **274**, 25026–25032
  9. Lee, M. S., and Mariani, K. J. (1987) *Escherichia coli* replication factor Y, a component of the primosome can act as a DNA helicase as a DNA helicase. *Proc. Natl. Acad. Sci. U.S.A.* **84**, 8345–8349
  10. Jones, J. M., and Nakai, H. (1999) Duplex opening by primosome protein PriA for replisome assembly on a recombination intermediate. *J. Mol. Biol.* **289**, 503–516
  11. Zavitz, K. H., and Mariani, K. J. (1992) ATPase-deficient mutants of the *Escherichia coli* DNA replication protein PriA are capable of catalyzing the assembly of active primosomes. *J. Biol. Chem.* **267**, 6933–6940
  12. Xu, L., and Mariani, K. J. (2003) PriA mediates DNA replication pathway choice at recombination intermediates. *Mol. Cell* **11**, 817–826
  13. Yuan, Q., and McHenry, C. S. (2009) Strand displacement by DNA polymerase III occurs through a  $\tau$ - $\psi$ - $\chi$  link to SSB coating the lagging strand template. *J. Biol. Chem.* **284**, 31672–31679
  14. Lopper, M., Boonsombat, R., Sandler, S. J., and Keck, J. L. (2007) A hand-off mechanism for primosome assembly in replication restart. *Mol. Cell* **26**, 781–793
  15. Mok, M., and Mariani, K. J. (1987) The *Escherichia coli* preprimosome and DNA B helicase can form replication forks that move at the same rate. *J. Biol. Chem.* **262**, 16644–16654
  16. Wu, C. A., Zechner, E. L., and Mariani, K. J. (1992) Coordinated leading and lagging-strand synthesis at the *Escherichia coli* DNA replication fork. I. multiple effectors act to modulate okazaki fragment size. *J. Biol. Chem.* **267**, 4030–4044
  17. Zechner, E. L., Wu, C. A., and Mariani, K. J. (1992) Coordinated leading and lagging-strand synthesis at the *Escherichia coli* DNA replication fork. II. frequency of primer synthesis and efficiency of primer utilization control okazaki fragment size. *J. Biol. Chem.* **267**, 4045–4053
  18. Kim, S., Dallmann, H. G., McHenry, C. S., and Mariani, K. J. (1996) Coupling of a replicative polymerase and helicase: a  $\tau$ -DnaB interaction mediates rapid replication fork movement. *Cell* **84**, 643–650
  19. Marsin, S., McGovern, S., Ehrlich, S. D., Bruand, C., and Polard, P. (2001) Early steps of *Bacillus subtilis* primosome assembly. *J. Biol. Chem.* **276**, 45818–45825
  20. Smits, W. K., Goranov, A. I., and Grossman, A. D. (2010) Ordered association of helicase loader proteins with the *Bacillus subtilis* origin of replication *in vivo*. *Mol. Microbiol.* **75**, 452–461
  21. Sanders, G. M., Dallmann, H. G., and McHenry, C. S. (2010) Reconstitution of the *B. subtilis* replisome with 13 proteins including two distinct replicases. *Mol. Cell* **37**, 273–281
  22. Bjornson, K. P., Amaratunga, M., Moore, K. J., and Lohman, T. M. (1994) Single-turnover kinetics of helicase-catalyzed DNA unwinding monitored continuously by fluorescence energy transfer. *Biochemistry* **33**, 14306–14316
  23. Houston, P., and Kodadek, T. (1994) Spectrophotometric assay for enzyme-mediated unwinding of double-stranded DNA. *Proc. Natl. Acad. Sci. U.S.A.* **91**, 5471–5474
  24. Kim, D. R., and McHenry, C. S. (1996) *In vivo* assembly of overproduced DNA polymerase III: Overproduction, purification, and characterization of the  $\alpha$ ,  $\alpha$ - $\epsilon$ , and  $\alpha$ - $\epsilon$ - $\theta$  subunits. *J. Biol. Chem.* **271**, 20681–20689
  25. Wiczorek, A., and McHenry, C. S. (2006) The NH(2)-terminal php domain of the  $\alpha$  subunit of the *E. coli* replicase binds the  $\epsilon$  proofreading subunit. *J. Biol. Chem.* **281**, 12561–12567
  26. Dallmann, H. G., Thimmig, R. L., and McHenry, C. S. (1995) DnaX complex of *Escherichia coli* DNA polymerase III holoenzyme: Central role of  $\tau$  in initiation complex assembly and in determining the functional asymmetry of holoenzyme. *J. Biol. Chem.* **270**, 29555–29562
  27. Song, M. S., Pham, P. T., Olson, M., Carter, J. R., Franden, M. A., Schaaper, R. M., and McHenry, C. S. (2001) The  $\delta$  and  $\delta'$  subunits of the DNA polymerase III holoenzyme are essential for initiation complex formation and processive elongation. *J. Biol. Chem.* **276**, 35165–35175
  28. Olson, M. W., Dallmann, H. G., and McHenry, C. S. (1995) DnaX-complex of *Escherichia coli* DNA polymerase III holoenzyme: The  $\chi\psi$  complex functions by increasing the affinity of  $\tau$  and  $\gamma$  for  $\delta$ - $\delta'$  to a physiologically relevant range. *J. Biol. Chem.* **270**, 29570–29577
  29. Johanson, K. O., Haynes, T. E., and McHenry, C. S. (1986) Chemical characterization and purification of the  $\beta$  subunit of the DNA polymerase III holoenzyme from an overproducing strain. *J. Biol. Chem.* **261**, 11460–11465
  30. Griep, M. A., and McHenry, C. S. (1989) Glutamate overcomes the salt inhibition of DNA polymerase III holoenzyme. *J. Biol. Chem.* **264**, 11294–11301
  31. Mariani, K. J. (1995) phi X174-Type primosomal proteins: Purification and assay. *Methods Enzymol.* **262**, 507–521
  32. Fijalkowska, I. J., and Schaaper, R. M. (1996) Mutants in the Exo I motif of *Escherichia coli* dnaQ: defective proofreading and inviability due to error catastrophe. *Proc. Natl. Acad. Sci. U.S.A.* **93**, 2856–2861
  33. Dallmann, H. G., Fackelmayer, O. J., Tomer, G., Chen, J., Wiktor-Becker, A., Ferrara, T., Pope, C., Oliveira, M. T., Burgers, P. M., Kaguni, L. S., and McHenry, C. S. (2010) Parallel multiplicative target screening against divergent bacterial replicases: Identification of specific inhibitors with broad spectrum potential. *Biochemistry* **49**, 2551–2562
  34. Heller, R. C., and Mariani, K. J. (2005) The disposition of nascent strands at stalled replication forks dictates the pathway of replisome loading during restart. *Mol. Cell* **17**, 733–743
  35. Xi, J., Zhuang, Z., Zhang, Z., Selzer, T., Spiering, M. M., Hammes, G. G., and Benkovic, S. J. (2005) Interaction between the T4 helicase-loading protein (gp59) and the DNA polymerase (gp43): A locking mechanism to delay replication during replisome assembly. *Biochemistry* **44**, 2305–2318
  36. Condon, C. (2003) RNA processing and degradation in *Bacillus subtilis*. *Microbiol. Mol. Biol. Rev.* **67**, 157–174, table of contents
  37. McHenry, C. S. (2011) Breaking the rules: bacteria that use several DNA polymerase IIIs. *EMBO Rep.* **12**, 408–414
  38. Dervyn, E., Suski, C., Daniel, R., Bruand, C., Chapuis, J., Errington, J., Janni re, L., and Ehrlich, S. D. (2001) Two essential DNA polymerases at the bacterial replication fork. *Science* **294**, 1716–1719
  39. Bruand, C., Farache, M., McGovern, S., Ehrlich, S. D., and Polard, P. (2001) DnaB, DnaD and DnaI proteins are components of the *Bacillus subtilis* replication restart primosome. *Mol. Microbiol.* **42**, 245–255
  40. Lisal, J., Lam, T. T., Kainov, D. E., Emmett, M. R., Marshall, A. G., and Tuma, R. (2005) Functional visualization of viral molecular motor by hydrogen-deuterium exchange reveals transient states. *Nat. Struct. Mol. Biol.* **12**, 460–466
  41. Sandler, S. J., Mariani, K. J., Zavitz, K. H., Coutu, J., Parent, M. A., and Clark, A. J. (1999) dnaC mutations suppress defects in DNA replication- and recombination-associated functions in *priB* and *priC* double mutants in *Escherichia coli* K-12. *Mol. Microbiol.* **34**, 91–101
  42. Bruand, C., Velten, M., McGovern, S., Marsin, S., S er en, C., Ehrlich, S. D., and Polard, P. (2005) Functional interplay between the *Bacillus subtilis* DnaD and DnaB proteins essential for initiation and re-initiation of DNA replication. *Mol. Microbiol.* **55**, 1138–1150
  43. Kaplan, D. L., and Steitz, T. A. (1999) DnaB from *Thermus aquaticus* unwinds forked duplex DNA with an asymmetric tail length dependence. *J. Biol. Chem.* **274**, 6889–6897
  44. Cadman, C. J., and McGlynn, P. (2004) PriA helicase and SSB interact physically and functionally. *Nucleic Acids Res.* **32**, 6378–6387
  45. Costes, A., Leco te, F., McGovern, S., Quevillon-Cheruel, S., and Polard, P. (2010) The C-terminal domain of the bacterial SSB protein acts as a DNA maintenance hub at active chromosome replication forks. *PLoS Genet.* **6**, e1001238

SUPPLEMENTAL MATERIAL FOR

**The PriA Replication Restart Protein Blocks Replicase Access and Directs**

**Template Specificity through its ATPase Activity**

Carol M. Manhart and Charles S. McHenry

**Supplemental TABLE S1. Determining the minimal substrate to sustain efficient helicase loading.**

Regions of the substrate in Fig. 1 were varied to determine the minimal substrate that can support an efficient helicase loading reaction. A replication fork consisting of a 45-mer lagging strand arm, a 45-mer parental duplex region, a 35-mer leading strand duplex region, and a 10 nucleotide gap are constructed from FT90, QT90, and P10g. Where regions were shortened, the sequences given in Fig. 1E were truncated from this starting substrate.

*Varying lagging strand arm with 10 nt gap on leading strand*

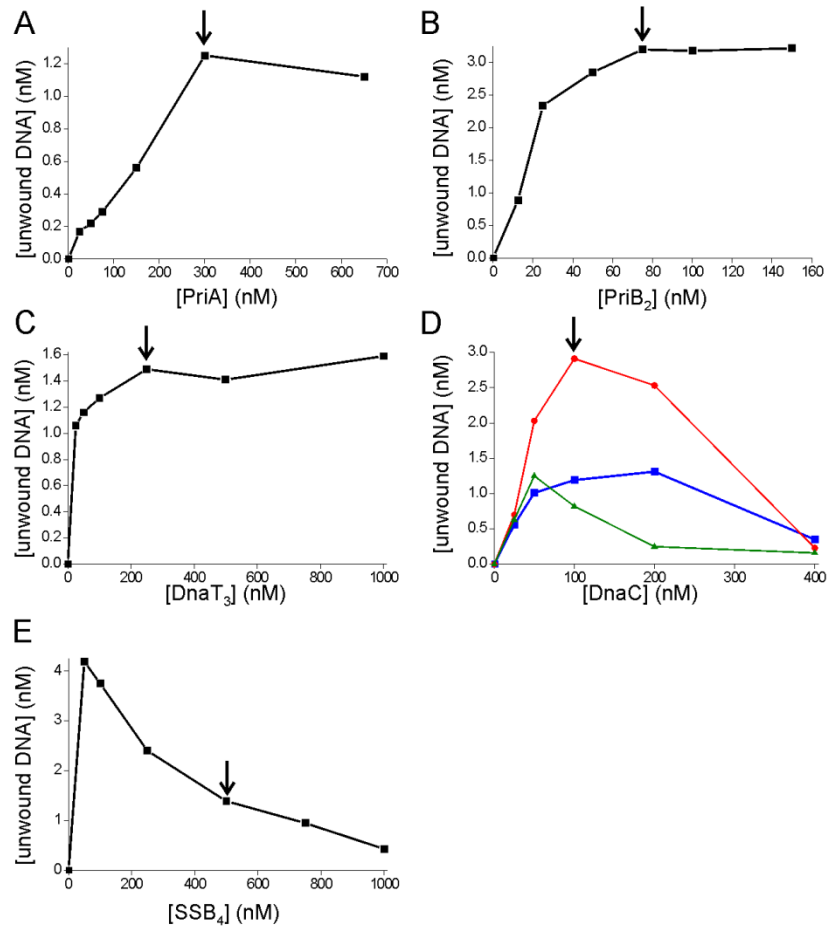
<b>Lagging Strand Arm Length (nt)</b>	<b>[unwound DNA] (nM) in <i>Bsu</i></b>	<b>[unwound DNA] (nM) in <i>Eco</i></b>
45	7.5	7.1
35	5.1	6.1
25	3.2	3.6
15	0.0	0.9
5	0.0	0.0

*Varying parental duplex region with 10 nt gap on leading strand*

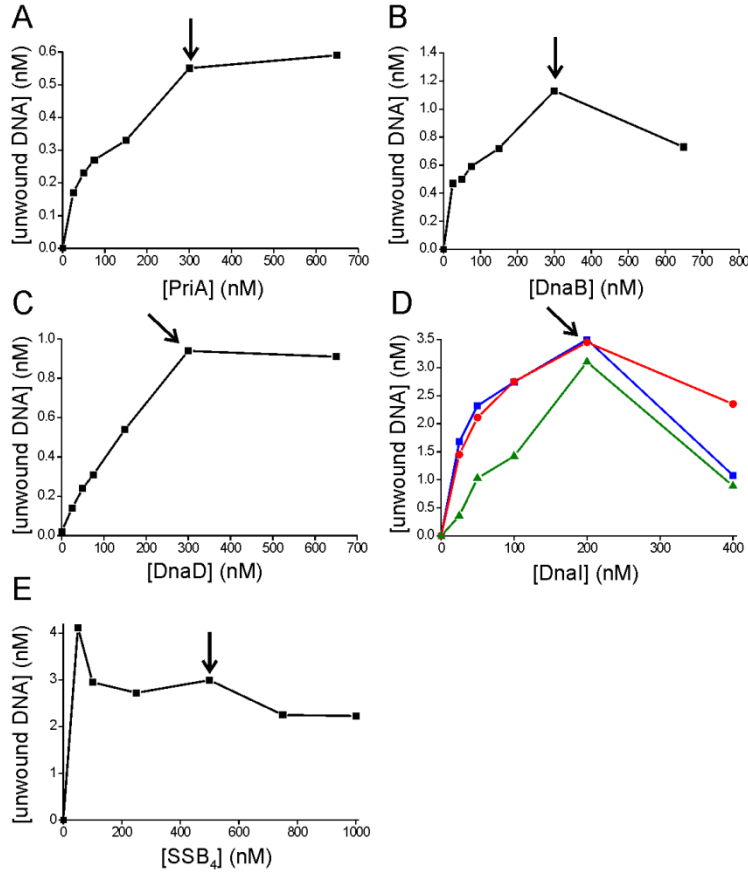
<b>Parental Duplex Length (nt)</b>	<b>[unwound DNA] (nM) in <i>Bsu</i></b>	<b>[unwound DNA] (nM) in <i>Eco</i></b>
45	7.5	7.1
30	3.9	3.0

*Varying leading strand duplex region with 10 nt gap on leading strand*

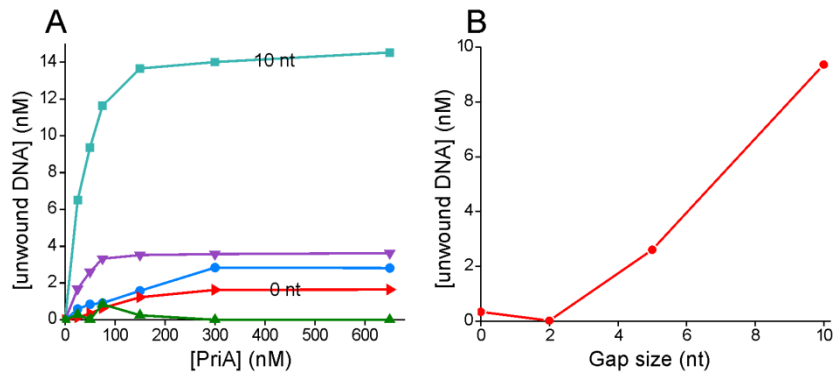
<b>Leading Strand Duplex Length (nt)</b>	<b>[unwound DNA] (nM) in <i>Bsu</i></b>	<b>[unwound DNA] (nM) in <i>Eco</i></b>
35	7.5	7.1
30	0.0	0.3



**SUPPLEMENTAL FIGURE S1. Optimization of *E. coli* helicase loading on 20 nM 0 nt gap forked template.** Experiments were carried out as in Fig. 3. The starting conditions were: 50 nM PriB<sub>2</sub>, 333 nM DnaT<sub>3</sub>, 12 nM DnaB<sub>6</sub>, 108 nM DnaC, and 500 nM SSB<sub>4</sub>. The final optimized conditions (indicated by arrows) were: 300 nM PriA, 75 nM PriB<sub>2</sub>, 250 nM DnaT<sub>3</sub>, 12 nM DnaB<sub>6</sub>, 100 nM DnaC, and 500 nM SSB<sub>4</sub>. *A*, PriA titration. *B*, PriB<sub>2</sub> titration. *C*, DnaT<sub>3</sub> titration. *D*, DnaC titrated at three different DnaB<sub>6</sub> concentrations: 6 nM (green), 12 nM (red), and 24 nM (blue). *E*, SSB<sub>4</sub> titration. To prevent the helicase self-loading reaction, 500 nM SSB<sub>4</sub> was chosen for future experiments.

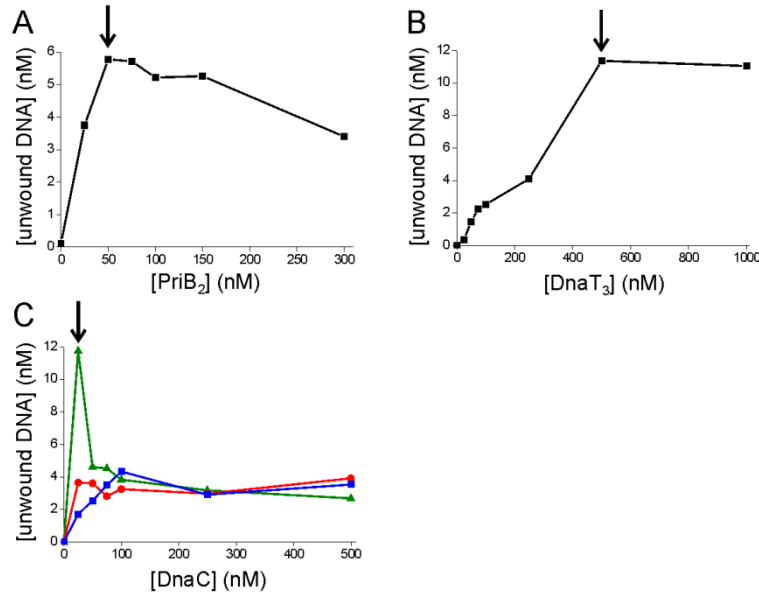


**SUPPLEMENTAL FIGURE S2. Optimizing *B. subtilis* helicase loading on 20 nM 0 nt gap forked template.** Experiments were carried out as in Fig. 3. The starting conditions were: 300 nM DnaB, 300 nM DnaD, 12 nM DnaC<sub>6</sub>, 100 nM DnaI, and 500 nM SSB<sub>4</sub>. The final optimized conditions (indicated by arrows) were: 300 nM PriA, 300 nM DnaB, 300 nM DnaD, 12 nM DnaC<sub>6</sub>, 200 nM DnaI and 500 nM SSB<sub>4</sub>. A, PriA titration. B, DnaB titration. C, DnaD titration. D, DnaI titrated at three different DnaC<sub>6</sub> concentrations: 6 nM (green), 12 nM (red), and 24 nM (blue). E, SSB<sub>4</sub> titration. To prevent the helicase self-loading reaction, 500 nM SSB<sub>4</sub> was used for future experiments.

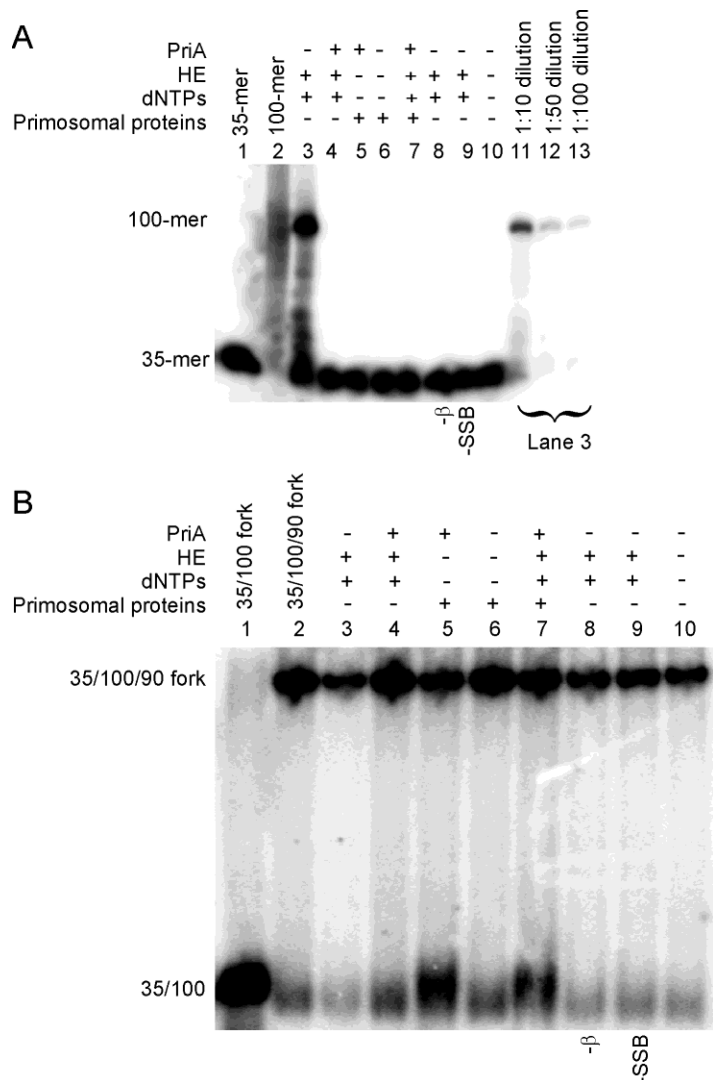


**SUPPLEMENTAL FIGURE S3. A larger gap on the leading strand is also preferred using the *E. coli* system under conditions optimized for the 0 nt gap forked template.** Protein concentrations were those described in the legend to supplemental Fig. S1. A, PriA titration on five unique substrates:

unprimed forked template (blue), 0 nt gap forked template (red), 2 nt gap forked template (green), 5 nt gap forked template (purple), or 10 nt gap forked template (cyan). *B*, Amount of DNA unwound plotted against gap size at 50 nM PriA.



**SUPPLEMENTAL FIGURE S4. Optimization of protein levels on forked template bound to streptavidin beads.** Radiolabeled, biotinylated primer/10 nt gap forked template was bound to streptavidin beads as described under *Experimental Procedures*. After washing, the substrate (20 nM final concentration) was incubated with 2 mM ATP, 500 nM PriA, 500 nM SSB<sub>4</sub>, and helicase and helicase-loading proteins for 15 min at room temperature. The reaction was quenched and the product was removed from the beads. The sample was resolved by 12 % native PAGE. PriA and SSB<sub>4</sub> were held constant at 500 nM. The remaining proteins were titrated sequentially in the order they appear here. For each, an optimum was chosen (as indicated by the arrow) and that concentration was used in subsequent titrations. The starting conditions for titration of the other helicase loading proteins and helicase were: 333 nM DnaT<sub>3</sub>, 40 nM DnaB<sub>6</sub>, and 200 nM DnaC. The final optimized conditions were: 50 nM PriB<sub>2</sub>, 500 nM DnaT<sub>3</sub>, 12 nM DnaB<sub>6</sub>, and 25 nM DnaC. *A*, PriB<sub>2</sub> titration. *B*, DnaT<sub>3</sub> titration. *C*, DnaC titrated at three different DnaB<sub>6</sub> concentrations: 12 nM (green), 40 nM (red), and 80 nM (blue).



**SUPPLEMENTAL FIGURE S5. PriA and holoenzyme do not coexist on PriA-inhibited replication forks with a 20 nt gap.** Substrate constructed from biotinylated primer 20 nt gap 5'-

CT(biotin)ACGATCATTGGAAGATTCTTACATTAGCCGACA-3', FT<sub>100</sub>, and lagging strand template 90-mer. This experiment carried out as described for reactions on streptavidin beads under *Experimental Procedures* and in the legend for Fig. 7. *A*, Denaturing gel analysis to monitor primer extension by *E. coli* Pol III (exo-). *Lanes 11-13* are dilutions of the positive control lane 3 to establish detection limits.

For both *A* and *B*, *lanes 8 and 9* contain the full Pol III HE but in *lane 8* the  $\beta_2$  subunit was omitted and in *lane 9* SSB was omitted. *B*, Native gel analysis to monitor substrate unwinding by *E. coli* DnaB helicase. The upper band is the replication fork and 100/100 duplex for those reactions in which replication occurred. The lower band is the displaced leading strand primer-template. In *lanes 5 and 7* ~50 % of the substrate was unwound by the helicase. In all other lanes, the amount of substrate unwound is not significantly above background.

# The PriA Replication Restart Protein Blocks Replicase Access Prior to Helicase Assembly and Directs Template Specificity through Its ATPase Activity

Carol M. Manhart and Charles S. McHenry

*J. Biol. Chem.* 2013, 288:3989-3999.

doi: 10.1074/jbc.M112.435966 originally published online December 20, 2012

---

Access the most updated version of this article at doi: [10.1074/jbc.M112.435966](https://doi.org/10.1074/jbc.M112.435966)

#### Alerts:

- [When this article is cited](#)
- [When a correction for this article is posted](#)

[Click here](#) to choose from all of JBC's e-mail alerts

#### Supplemental material:

<http://www.jbc.org/content/suppl/2012/12/20/M112.435966.DC1.html>

This article cites 45 references, 23 of which can be accessed free at <http://www.jbc.org/content/288/6/3989.full.html#ref-list-1>